Original Research

Value of Delayed Hypointensity and Delayed Enhancing Rim in Magnetic Resonance Imaging Diagnosis of Small Hepatocellular Carcinoma in the Cirrhotic Liver

Asra S. Khan, MD,[1]* Hero K. Hussain, MD,[1] Timothy D. Johnson, PhD,[2] William J. Weadock, MD,[1] Shawn J. Pelletier, MD,[3] and Jorge A. Marrero, MD, MS[4]

Purpose: To determine the diagnostic utility of delayed hypointensity and delayed enhancing rim on magnetic resonance imaging (MRI) as indicators of hepatocellular carcinoma (HCC) in arterially enhancing nodules ≤5 cm in the cirrhotic liver and determine the features that best predict HCC.

Materials and Methods: Gadolinium-enhanced MRI studies performed from January 2001 to December 2004 in patients with cirrhosis were evaluated for arterially enhancing nodules measuring ≤5 cm. Verification was via explant correlation, biopsy, or imaging follow-up. Sensitivity and specificity of diagnostic features of HCC were calculated. Features predictive of HCC were determined using the Generalized Estimating Equation approach.

Results: In all, 116 arterially enhancing nodules were identified in 80 patients (<2 cm: $n = 79$, 2–5 cm $n = 37$). Sensitivity and specificity of delayed hypointensity for HCC measuring ≤5 cm, 2–5 cm, and <2 cm were 0.54 (40 of 74) and 0.86 (36 of 42); 0.72 (23 of 32) and 0.80 (4 of 5); and 0.41 (17 of 42) and 0.87 (32 of 37). For the delayed enhancing rim sensitivity and specificity were 0.64 (47 of 74) and 0.86 (36 of 42); 0.75 (24 of 32) and 1.0 (5 of 5); and 0.55 (23 of 42) and 0.83 (31 of 37), respectively. Lesion size (≥2 cm) and delayed enhancing rim, as main features and their interaction, were the most significant predictors of HCC.

Conclusion: Delayed hypointensity and enhancing rim improve the specificity of diagnosis of HCC of all sizes but are seen less frequently in small (<2 cm) HCC. Nodule size (≥2 cm) and delayed enhancing rim are the strongest predictors of HCC.

Key Words: liver; hepatocellular carcinoma; cirrhosis
J. Magn. Reson. Imaging 2010;32:360–366.

HEPATOCELLULAR CARCINOMA (HCC) is the most common primary hepatic malignancy, with an incidence in the United States of 2.4 per 100,000 per year (1). Liver transplantation can markedly increase survival in patients with HCC if criteria for early staging are met (2,3). Current United Network of Organ Sharing (UNOS) criteria for transplantation do not require tissue confirmation of HCC by biopsy but rely on imaging characterization, particularly arterial enhancement (4). However, pretransplant image staging has been shown to be less then 50% accurate when compared to posttransplant pathological staging with imaging over- and understaging HCC (5).

Due to the scarcity of livers available it is imperative to accurately characterize focal liver lesions prior to transplantation. However, using the current UNOS criteria of arterial blush, at a single transplant center in the United States, 33% of patients transplanted for HCC did not have tumor in the explant and 63% of the misdiagnosed tumors were arterially enhancing lesions 2 cm or smaller in diameter (6). Moreover, studies have shown that up to 93% of lesions less than 2 cm seen only on the arterial phase of imaging are nonneoplastic (7–11). Thus, arterial enhancement alone is not always specific for HCC (12).

Patients with limited HCC (TNM stage II: single HCC 2–5 cm or up to 3 HCCs, each less than 3 cm) can undergo liver transplantation. Single small HCC (<2 cm) can be successfully treated with resection or ablation and are more likely to have complete response to local therapies (13).

Hypointensity on portal venous and/or delayed phases of gadolinium-enhanced imaging has been reported as a specific indicator of HCC (14–16).

[1]Department of Radiology, University of Michigan, Ann Arbor, Michigan, USA.
[2]Department of Biostatistics, University of Michigan, Ann Arbor, Michigan, USA.
[3]Department of Surgery, University of Michigan, Ann Arbor, Michigan, USA.
[4]Department of Gastroenterology, University of Michigan, Ann Arbor, Michigan, USA.
*Address reprint requests to: A.S.K., Dept. of Radiology, University of Michigan, 1500 E. Medical Center Dr., Ann Arbor MI 48109. E-mail: Asrakhan68@gmail.com
Received December 14, 2009; Accepted April 29, 2010.
DOI 10.1002/jmri.22271
Published online in Wiley InterScience (www.interscience.wiley.com).

However, small histologically well-differentiated "early HCC" may retain some conventional liver vasculature, and consequently not demonstrate delayed hypointensity (17). Delayed enhancing rim is also a known feature of HCC (18–20). Few studies have investigated the frequency of occurrence of delayed hypointensity or delayed enhancing rim in HCC in the cirrhotic liver.

The purpose of this study was to determine the diagnostic utility of delayed hypointensity and delayed enhancing rim on MRI as indicators of HCC in arterially enhancing nodules ≤5 cm in the cirrhotic liver and to determine the features that best predict HCC.

MATERIALS AND METHODS

This retrospective study was in compliance with our Institutional Review Board (IRB) rules and the Health Insurance Portability and Accountability Act (HIPAA). IRB approval was obtained for the study and informed consent waived due to its retrospective nature.

Study Population

Our hospital MRI records were searched for all adults (≥18 years) with chronic liver disease who underwent liver MRI between January 2001 and December 2004. Changes of cirrhosis were confirmed by histology in 64 patients (43 percutaneous biopsies, 21 explants). In 12 patients pathologic confirmation was not available; however, morphological changes of cirrhosis and secondary portal hypertension were seen on MRI. In the four remaining patients, biopsy demonstrated fibrosis and inflammation without frank changes of cirrhosis. As screening is recommended in patients with bridging fibrosis (18) because transition from bridging fibrosis to cirrhosis is difficult to determine clinically, these patients were included in our study.

For inclusion, the patient must have had diagnostic quality contrast-enhanced 3D T1-weighted gradient-recalled echo (GRE) imaging with the arterial-dominant phase ideally timed (enhancement of hepatic arteries, slight enhancement of portal vein, and no enhancement of hepatic veins). However, if timing was earlier with minimal or no portal vein enhancement ($n = 4$), the patient was still included, as an enhancing nodule would accumulate contrast sooner than surrounding parenchyma. Studies that showed enhancement of the hepatic veins on the first phase of imaging were excluded.

Patients with known HCC who underwent partial hepatectomy or radiofrequency ablation were included and evaluated for additional lesions. Those treated with transarterial chemoembolization (TACE) or radiation therapy were excluded as these treatments may change the perfusion dynamics of the liver.

A total of 394 patients with cirrhosis and available verification of MRI findings were scanned from January 2001 to December 2004. In all, 274 patients were excluded because of no visualized arterially enhancing nodule ≤5 cm, nine for suboptimal dynamic phase imaging (missed arterial phase imaging $n = 4$; nondiagnostic study $n = 5$), and 31 for prior therapy (TACE $n = 22$, radiotherapy $n = 9$). Thus, the study population comprised 80 patients (mean age 57 years, range 36–78) with 116 arterially enhancing nodules measuring ≤5 cm. Twenty patients were women (mean age 59.4 years, range 36–78 years) and 60 were men (mean age 55.3 years, range 41–74 years). Fifty-six patients had one arterially enhancing nodule, 12 had two, and 12 had three.

MRI Techniques

MR imaging was performed on a 1.5-T system (Signa; General Electric Medical Systems, Milwaukee, WI). A 4-channel phased array receiver coil was used. T1-W imaging included dual-echo opposed-phase (OP)/in-phase (IP) GRE imaging (TR/TE <180/2.2–4.4 msec, flip angle 70°, slice thickness/gap 6/0 mm, matrix 256 (frequency) × 160 (phase)). T2-W imaging was performed using either a fat-suppressed respiratory-triggered fast spin-echo (FSE) sequence (TR range/TE_{eff} <5000/80–100 msec, echo train length 18) ($n = 54$ patients) or a breath hold fast recovery FSE (FR-FSE) sequence (TR range/TE_{eff} <2500/80–100 msec, echo train length 17) ($n = 26$ patients), slice thickness/gap 6/0 mm, matrix 256 × 224. A rectangular field of view was often used to reduce the number of phase-encoding acquisitions.

Dynamic imaging was performed before and after intravenous injection of gadopentetate dimeglumine (Magnevist; Bayer, Wayne, NJ) using a 3D GRE sequence with spectral fat saturation (TR/TE 4–6/1.2 msec, flip angle 12°, matrix 256–320 × 128–192, section thickness 4.0 mm with 2 mm overlap). Gadopentetate dimeglumine was used at a dose of 0.1 mmol/kg (maximum dose 20 mL) administered via a power injector in an antecubital vein at a rate of 2 mL/sec, followed by 20 mL of normal saline flush at the same rate. After unenhanced imaging, contrast arrival for arterial-dominant phase imaging were timed using automated contrast bolus detection, Smart-Prep (GE Medical Systems). Venous and extracellular phase images were obtained at ≈50–70 sec and 120–200 sec, respectively, after the initiation of contrast injection.

Image Analysis

Studies were reviewed independently by two radiologists with 4 and 10 years experience interpreting liver MRI on a commercially available workstation (Advantage Workstation; GE Medical Systems). Lesions were preselected for review by one reader who noted the image number of the lesion on the arterial phase of postgadolinium imaging. If the second reviewer noted an additional lesion then the discrepancy was resolved by consensus ($n = 2$). All sequences for each study were presented to the reviewers in one setting. Readers were blinded to the clinical MRI interpretations and final diagnosis.

Arterially enhancing nodules measuring ≤5 cm were identified (Fig. 1a). Comparison to precontrast fat-suppressed T1-weighted sequence was made to ensure that hyperintensity was due to contrast enhancement and subtraction imaging (arterial-phase

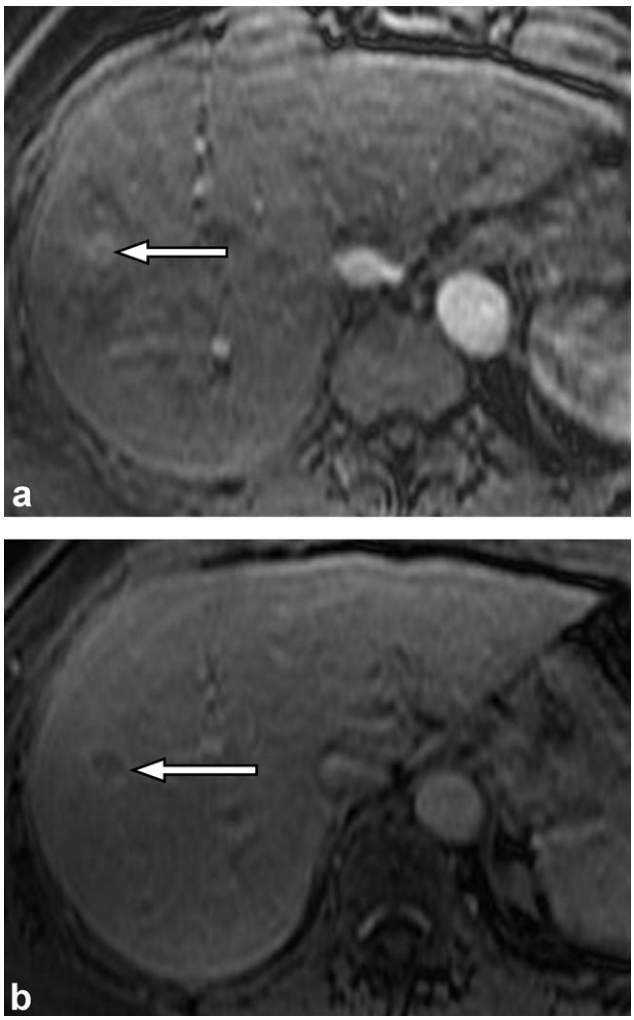

Figure 1. A 31-year-old woman with hepatitis C cirrhosis. (**a**) T1-weighted volumetric 3D fat-suppressed spoiled gradient echo MR image (TR/TE, 4–6/1.2 msec flip angle 12°) in the arterial phase demonstrating a small enhancing nodule (arrow). (**b**) MR images obtained in the extracellular phase show hypointensity and a peripheral capsule.

minus precontrast) was occasionally performed for lesions (n = 17) with hyperintense signal on precontrast imaging. For patients with multiple lesions the three largest lesions within this size limit were included. Both radiologists assigned a qualitative assessment score of lesion signal intensity with respect to the background liver as hyperintense, isointense, or hypointense. Lesion signal intensity was recorded on T1-W OP/IP, T2-W, and gadolinium-enhanced sequences. Any interpretation discrepancy (n = 6) was resolved by reassessment of lesion signal intensity relative to adjacent parenchyma by consensus of the two radiologists. Other findings of rim enhancement in the venous and/or delayed phases (Fig. 1b), and internal lipid, identified by comparing in-phase and out-of-phase T1-W imaging were also documented.

Verification

Verification of the identified lesions with pathology (explant or biopsy) or follow-up MRI was essential for inclusion. Lesions that demonstrated interval growth of 100% diameter increase in 1 year or 50% in 6 months (21) or had pathological confirmation were considered HCC. For classification as nonmalignant, lesions had to have pathological proof of diagnosis or at least 18-month MRI follow-up demonstrating stability or disappearance.

Explanted livers were cut sequentially in 5–10-mm sections in the axial plane to match the MRI studies. The MRI reports were reviewed at time of gross sectioning to guide nodule localization. The overall mean time between transplant and MRI was 7.2 months (range 1–33) including 13.1 months (range 1–33) for 14 nonmalignant lesions and 4.4 months (range 1–18) for 29 malignant lesions.

Of the 116 lesions included in the study, verification was by biopsy for 28, explant correlation for 43, and MRI follow-up for 45 lesions (mean 20.4, range 4–47).

Statistical Analysis

Sensitivity and specificity of delayed hypointensity and delayed enhancing rim, as features diagnostic of HCC, were calculated on a lesion-by-lesion basis. Generalized Estimating Equations (GEE) (22) models were fit with the main imaging features of HCC and their interactions to determine the predictors of HCC. GEE is a statistical method that fits parameters to a generalized linear model when unknown correlation is present. The focus of a GEE analysis is on population level average effects rather than random effects. The main features were: size 2 cm or larger and less than 2 cm, T2-weighted hyperintense signal, T1-weighted hypointense signal, lipid content, delayed postcontrast hypointensity, and delayed enhancing rim. The sampling took place at the patient level, with clusters of lesions within individuals. Leaving one variable out at a time cross-validation was used to estimate sensitivity and specificity of the resulting models.

RESULTS

Of the 116 nodules included in the study, 74 (64%) were HCC (transplant n = 29, biopsy n = 22, MRI follow-up n = 23) and 42 were nonmalignant.

Of the 42 nonmalignant arterially enhancing nodules, 20 were verified at pathology (explant n = 14 [12 regenerative nodules and two high-grade dysplastic nodules]; biopsy n = 6 [two regenerative nodules, two high-grade dysplastic nodules, one fibrosis, and one focal nodular hyperplasia]) and 22 by follow-up MRI for a minimum of 18 months (mean 27.5, range 19–47).

Mean size of 74 HCC nodules was 2.2 cm (range 1.0–4.8 cm) and that of nonmalignant nodules 1.5 cm (1.0–4.6 cm). 32 of 74 (43%) HCC nodules measured 2–5 cm and 42 (57%) were smaller than 2 cm. For one patient with three nodules, evaluation of unenhanced T1-W and T2-W signal intensity was not possible secondary to motion artifact. Of 113 nodules with diagnostic T2-W imaging 56 were isointense in signal relative to liver parenchyma (HCC n = 25; nonmalignant

Table 1
Sensitivity and Specificity of Delayed Hypointensity and Delayed Enhancing Rim as Features of Arterially Enhancing HCC ≤5 cm

Size [cm] Parameter	Sensitivity	Specificity
≤5		
Delayed hypointensity	0.54 (40/74)	0.86 (36/42)
Delayed enhancing rim	0.64 (47/74)	0.86 (36/42)
2-5		
Delayed hypointensity	0.72 (23/32)	0.80 (4/5)
Delayed enhancing rim	0.75 (24/32)	1.00 (5/5)
<2		
Delayed hypointensity	0.41 (17/42)	0.87 (32/37)
Delayed enhancing rim	0.55 (23/42)	0.83 (31/37)

$n = 31$) and 57 were hyperintense (HCC $n = 46$; nonmalignant $n = 11$). Internal fat was identified by demonstrating signal loss on out-of-phase imaging compared to in-phase and was seen in 14 nodules (HCC $n = 12$, nonmalignant $n = 2$).

Lesion-based sensitivities and specificities of delayed hypointensity and delayed enhancing rim for HCC are shown in Table 1. For analysis, hypointensity on either venous or delayed phase imaging was considered as delayed hypointensity. Delayed hypointensity was highly specific (0.87) for arterially enhancing HCC <2 cm but only seen in 17 of 42 (40%) of these small tumors. The 34 of 74 HCC in our study did not demonstrate delayed hypointensity including 25/42 <2 cm and 9/32 2–5 cm HCCs (Fig. 2). The sensitivity of delayed enhancing rim for HCC was slightly higher than that of delayed hypointensity, particularly for lesions <2 cm.

Four nonmalignant nodules demonstrated hypointensity on delayed phase imaging. Two of these nodules demonstrated no change on MRI follow-up over 26 and 35 months. Two had biopsy follow-up yielding one regenerative nodule and one regenerative nodule with small cell dysplasia.

Four nonmalignant lesions had a delayed enhancing rim. Two of these nodules were not seen on follow-up MRI done at 19 and 21 months. One was determined to be a high-grade dysplastic nodule at explant correlation. One had biopsy follow-up yielding high-grade dysplastic nodule.

Two benign lesions demonstrated both hypointensity and delayed enhancing rim. One lesion had biopsy yielding dysplastic nodule. One nodule had biopsy follow-up yielding fibrosis and 28-month MRI follow-up that demonstrated minimal change (Fig. 3).

A GEE model fitted with the individual features of HCC showed that delayed enhancing rim ($P = 0.026$) was a significant predictor of HCC (Table 2). To identify the best individual and combinations of features predictive of HCC, the least significant features were removed from the model (Table 3). The delayed enhancing rim and its interaction with size (≥2 cm) ($P = <2 \times 10^{-16}$) were the best predictors of HCC (Table 3).

DISCUSSION

HCC is thought to arise in the cirrhotic liver as a result of stepwise progression from regenerative nodule to low then high-grade dysplastic nodule, to dysplastic nodule with microscopic HCC, to small HCC. Imaging features reflect a shift in the dominant blood supply of these nodules as they progress to HCC (20). With progression to malignancy, the blood supply shifts from portal venous to abnormal hepatic arterial supply (neoplastic angiogenesis) resulting in arterial enhancement (23,24). Thus, arterial hypervascularity of a nodule is suspicious for HCC (25–27). However, arterial enhancement, especially in nodules measuring <2 cm, is nonspecific for HCC and is seen in nonmalignant lesions (23,28).

Since most arterially enhancing lesions ≥2 cm are highly likely to be HCC, current recommendations suggest that these lesions do not require pathological confirmation if they display imaging features typical for HCC (arterial hypervascularity and delayed hypointensity) on CT or MRI (9). Results from this study confirm that a high proportion (86%, 32/37) of arterially enhancing nodules measuring 2–5 cm are HCC.

Arterially enhancing lesions <2cm have a lower but still significant probability of being HCC. In this study, 53% (42/79) of such lesions were HCC. In the study by Marrero et al (16), 19% of arterially enhancing nodules <2 cm were HCC, and 23% (6 of 26) in the study by Jeong et al (21). At this level of

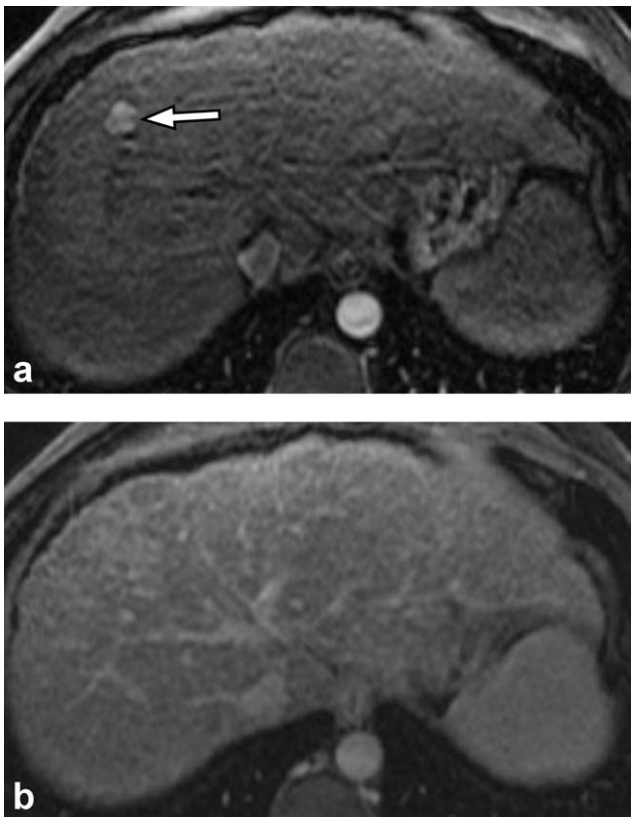

Figure 2. A 41-year-old man with hepatitis C and cirrhosis. (**a**) T1-weighted volumetric 3D fat-suppressed spoiled gradient echo MR image (TR/TE, 4–6/1.2 msec flip angle 12°) in the arterial phase demonstrating a small enhancing nodule (arrow). (**b**) MR images obtained in the extracellular phase show no hypointensity. However, at transplant this lesion was confirmed to be HCC.

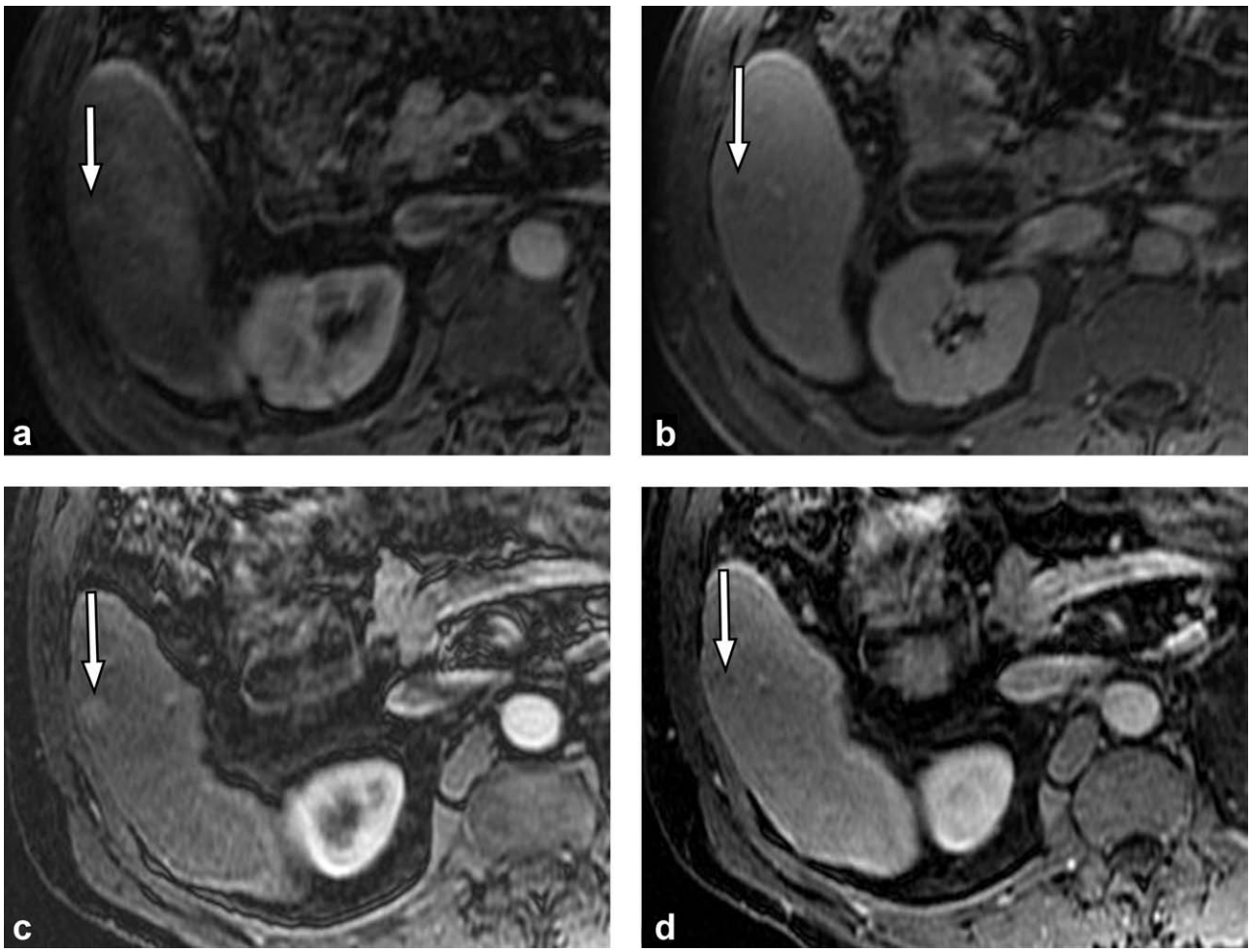

Figure 3. A 63-year-old man with hepatitis C and cirrhosis. (**a**) T1-weighted volumetric 3D fat-suppressed spoiled gradient echo MR image (TR/TE, 4–6/1.2 msec flip angle 12°) in the arterial phase demonstrating a small enhancing nodule (arrow). (**b**) MR images obtained in the extracellular phase show hypointensity and a peripheral enhancing rim. However, biopsy follow-up yielded chronic fibrosis. The perception of the capsule may be secondary to delayed enhancing fibrosis in the surrounding liver parenchyma. (**c,d**) A 28-month follow-up MRI demonstrates minimal change in lesion size.

incidence, more specific criteria for characterization of these nodules as HCC is needed.

Previous studies suggest that T2-W imaging does not provide additional diagnostic value compared to 3D gadolinium-enhanced imaging (29–31) for the diagnosis of HCC in the cirrhotic liver. Similar to other studies (32,33), our results suggest that T2-W imaging has better sensitivity in larger 2–5 cm lesions (0.80, 25/31) but decreases with smaller HCC <2 cm (0.53, 21/40).

As nodules progress to HCC and develop increasing arterial blood supply, there is a simultaneous decrease in their portal venous supply with resultant decreased enhancement during venous and extracellular phases

Table 2
P-values of All Main Imaging Features of HCC Fitted in the GEE Model to Predict HCC

Imaging variable	*P*-value
Size (<2 cm, ≥2 cm)	0.066
Delayed hypointensity	0.383
Delayed enhancing rim	0.026*
Internal lipid	0.880
T2-weighted hyperintensity	0.160
T1-weighted hypointensity	0.571

**P*-value equal to or less than 0.05 is statistically significant. Sensitivity: 0.732 (52/71) 95% CI (0.614, 0.831); specificity: 0.628 (27/42) 95% CI (0.480, 0.785).

Table 3
P-values of Main Imaging Features and Their Interactions Fitted in the GEE Model to Predict HCC

Imaging variables	*P*-value
Size (<2 cm, ≥2 cm)	0.325
Hypointensity	0.356
Rim	0.071
T2-weighted hyperintensity	0.070
Size × hypointensity	0.987
Size × rim	$<2 \times 10^{-16}$*
Size xT2-weighted hyperintensity	0.633

**P*-value equal to or less than 0.05 is statistically significant. Cross-validated sensitivity and specificity for this model: Sensitivity: 0.803 (57/71) 95% CI (0.691, 0.888); specificity: 0.619 (26/42) 95% CI (0.456, 0.764).

(34). Delayed hypointensity has been shown to be highly predictive of HCC. Marrero et al (16) showed sensitivity of 80% and specificity of 95% of delayed hypointensity for HCC in arterially enhancing nodules <2 cm, while Burrel et al (7) found arterial enhancement with delayed hypointensity to be 89% sensitive for HCC in 1–2 cm nodules. In our study, delayed hypointensity of arterially enhancing lesions <2 cm as an indicator for HCC was less sensitive at 41% (17/42) but demonstrated good specificity of 87% (32/37). For HCC measuring 2–5 cm, delayed hypointensity had a sensitivity of 72% (23/32) and specificity of 80% (4/5). The lower sensitivity in this study compared to previous work may be secondary to patient inclusion criteria. We included patients with biopsy and long-term MRI follow-up compared to Burrel et al (7), who included only explant patients, many of whom had known concomitant HCC possibly increasing the likelihood that visualized lesion was HCC. A study by Yu et al (35) which also included biopsy and MRI follow-up reported similar results for delayed hypointensity in HCC ≤2 cm with sensitivity of 43% and specificity of 89%.

In all, 34 of 74 HCC in our study did not demonstrate delayed hypointensity including 25/42 <2 cm and 9/32 2–5 cm HCCs. This likely relates to internal histological variations and possibly residual portal venous supply (20,34). Also, as portal venules have been suggested as the main drainage of HCC (36), immature portal venous drainage may prevent observation of delayed hypointensity.

The presence of a tumor capsule has been associated with the peripheral enhancing rim of HCC (14,17,34,35). This capsule is histologically composed of an inner layer of fibrous tissue and an outer layer of compressed vessels (17,34). The fibrous tissue will retain contrast longer than surrounding parenchyma, resulting in a delayed enhancing rim (35). This delayed rim enhancement has been shown to be highly specific for HCC in arterially enhancing lesions (14). A transient rim of enhancement in the venous phase, referred to as the "corona of HCC," is another possible cause for the peripheral enhancing rim. This is due to enhancement of compressed hepatic sinusoids surrounding the tumor. These sinusoids receive the portal venous drainage of HCC (36).

Comparing delayed hypointensity and delayed enhancing rim, our data suggest that the presence of a peripheral rim has slightly higher sensitivity but essentially similar specificity for the diagnosis of HCC of all sizes. Currently the AASLD emphasizes delayed hypointensity in the diagnosis of HCC, recommending that for 1–2 cm arterial hypervascular lesions, if hypointensity in the portal venous or delayed phase is confirmed on two dynamic studies, either CT scan, contrast ultrasound, or MRI with contrast, the lesion can be treated as HCC without pathological confirmation (15). However, our study shows that the delayed enhancing rim is a better predictor of HCC both as a main feature or in combination with size ≥2 cm as compared with delayed hypointensity.

Overall specificity of both delayed hypointensity and delayed enhancing rim was (0.86, 37/42) in this study. As biopsy verification of three of the lesions demonstrating hypointensity and two of the lesions with delayed enhancing rim yielded fibrosis, regenerative nodule or dysplastic nodule, sampling error could have increased the false-positive results. Also, as suggested by Yu et al (35), underlying fibrosis could also contribute to a false-positive rate since delayed hypointensity and delayed enhancing rim may be overestimated due to visual misperception caused by delayed enhancement of surrounding fibrotic parenchyma (Fig. 3a,b).

The study has several limitations. The study design is retrospective. The explanted livers were not always cut with the radiologist physically present but were always compared to the MRI report. Selection bias may have been introduced, as only lesions/patients suspicious for HCC were more likely be followed and hence be included in the study. As mentioned above, sampling error could have occurred in benign lesions verified by biopsy, leading to a false-negative diagnosis of HCC. Also, evaluation of imaging features was done qualitatively, and readers may have different thresholds for these features.

In conclusion, in arterially enhancing nodules of all sizes, delayed hypointensity improves the specificity of diagnosis of HCC but is frequently absent in very small HCC (<2 cm). Moreover, the presence of a delayed enhancing rim, irrespective of the presence of delayed hypointensity, is a strong predictor of HCC.

REFERENCES

1. El-Serag HB, Mason AC. Rising incidence of hepatocellular carcinoma in the United States. N Engl J Med 1999;340:745–750.
2. Mazzaferro V, Regalia E, Doci R, et al. Liver transplantation for the treatment of small hepatocellular carcinomas in patients with cirrhosis. N Engl J Med 1996;334:693–699.
3. Shetty K, Timmins K, Brensinger C, et al. Liver transplantation for hepatocellular carcinoma validation of present selection criteria in predicting outcome. Liver Transpl 2004;10:911–918.
4. UNOS. 3.6.4.4 Liver transplant candidates with hepatocellular carcinoma. In: Policies: 3.6 — Organ Distribution: Allocation of Livers Richmond, VA: United Network for Organ Sharing, 2008.
5. Freeman RB, Mithoefer A, Ruthazer R, et al. Optimizing staging for hepatocellular carcinoma before liver transplantation: a retrospective analysis of the UNOS/OPTN database. Liver Transpl 2006;12:1504–1511.
6. Hayashi PH, Trotter JF, Forman L, et al. Impact of pretransplant diagnosis of hepatocellular carcinoma on cadveric liver allocation in the era of MELD. Liver Transpl 2004;10:42–48.
7. Burrel M, Llovet JM, Ayuso C, et al. MRI angiography is superior to helical CT for detection of HCC prior to liver transplantation: an explant correlation. Hepatology 2003;38:1034–1042.
8. Mueller GC, Hussain HK, Carlos RC, Nghiem HV, Francis IR. Effectiveness of MR imaging in characterizing small hepatic lesions: routine versus expert interpretation. Am J Roentgenol 2003;180:673–680.
9. Bruix J, Sherman M. Management of hepatocellular carcinoma. Hepatology 2005;42:1208–1236.
10. Holland AE, Hecht EM, Hahn WY, et al. Importance of small (< or = 20-mm) enhancing lesions seen only during the hepatic arterial phase at MR imaging of the cirrhotic liver: evaluation and comparison with whole explanted liver. Radiology 2005;237:938–944.
11. Shimizu A, Ito K, Koike S, Fujita T, Shimizu K, Matsunaga N. Cirrhosis or chronic hepatitis: evaluation of small (< or = 2-cm) early-enhancing hepatic lesions with serial contrast-enhanced dynamic MR imaging. Radiology 2003;226:550–555.
12. Willatt JM, Hussain HK, Adusumilli S, Marrero JA. MR imaging of hepatocellular carcinoma in the cirrhotic liver: challenges and controversies. Radiology 2008;247:311–330.

13. Sala M, Llovet JM, Vilana R, et al. Initial response to percutaneous ablation predicts survival in patients with hepatocellular carcinoma. Hepatology 2004;40:1352–1360.
14. Carlos RC, Kim HM, Hussain HK, Francis IR, Nghiem HV, Fendrick AM. Developing a prediction rule to assess hepatic malignancy in patients with cirrhosis. Am J Roentgenol 2003;180: 893–900.
15. Ito K, Fujita T, Shimizu A, et al. Multiarterial phase dynamic MRI of small early enhancing hepatic lesions in cirrhosis or chronic hepatitis: differentiating between hypervascular hepatocellular carcinomas and pseudolesions. Am J Roentgenol 2004;183: 699–705.
16. Marrero JA, Hussain HK, Nghiem HV, Umar R, Fontana RJ, Lok AS. Improving the prediction of hepatocellular carcinoma in cirrhotic patients with an arterially enhancing liver mass. Liver Transpl 2005;11:281–289.
17. Efremidis SC, Hytiroglou P, Matsui O. Enhancement patterns and signal-intensity characteristics of small hepatocellular carcinoma in cirrhosis: pathologic basis and diagnostic challenges. Eur Radiol 2007;17:2969–2982.
18. Bruix J, Sherman M, Llovet JM, et al. Clinical management of hepatocellular carcinoma. Conclusions of the Barcelona-2000 EASL conference. European Association for the Study of the Liver. J Hepatol 2001;35:421–430.
19. Grazioli L, Olivetti L, Fugazzola C, et al. The pseudocapsule in hepatocellular carcinoma: correlation between dynamic MR imaging and pathology. Eur Radiol 1999;9:62–67.
20. Efremidis S, Hytiroglou P. The multistep process of hepatocarcinogenesis in cirrhosis with imaging correlation. Eur Radiol 2002; 12:753–764.
21. Jeong YY, Mitchell DG, Kamishima T. Small (<20 mm) enhancing hepatic nodules seen on arterial phase MR imaging of the cirrhotic liver: clinical implications. AJR Am J Roentgenol 2002; 178:1327–1334.
22. Zeger SL, Liang KY. Longitudinal data analysis for discrete and continuous outcomes. Biometrics 1986;42:121–130.
23. Krinsky GA, Theise ND, Rofsky NM, Mizrachi H, Tepperman LW, Weinreb JC. Dysplastic nodules in cirrhotic liver: arterial phase enhancement at CT and MR imaging—a case report. Radiology 1998;209:461–464.
24. Kageyama F, Kobayashi Y, Kawasaki T, et al. An unusual hyperplastic hepatocellular nodule in a patient with hepatitis C virus-related liver cirrhosis. Am J Gastroenterol 1998;93:2588–2593.
25. Yamashita Y, Mitsuzaki K, Yi T, et al. Small hepatocellular carcinoma in patients with chronic liver damage: prospective comparison of detection with dynamic MR imaging and helical CT of the whole liver. Radiology 1996;200:79–84.
26. Oi H, Murakami T, Kim T, Matsushita M, Kishimoto H, Nakamura H. Dynamic MR imaging and early-phase helical CT for detecting small intrahepatic metastases of hepatocellular carcinoma. AJR Am J Roentgenol 1996;166:369–374.
27. Yamashita Y, Fan ZM, Yamamoto H, et al. Spin-echo and dynamic gadolinium-enhanced FLASH MR imaging of hepatocellular carcinoma: correlation with histopathologic findings. J Magn Reson Imaging 1994;4:83–90.
28. Nakashima O, Kurogi M, Yamaguchi R, et al. Unique hypervascular nodules in alcoholic liver cirrhosis: identical to focal nodular hyperplasia-like nodules? J Hepatol 2004;41:992–998.
29. Fujita T, Ito K, Honjo K, Okazaki H, Matsumoto T, Matsunaga N. Detection of hepatocellular carcinoma: comparison of T2-weighted breath-hold fast spin-echo sequences and high-resolution dynamic MR imaging with a phased-array body coil. J Magn Reson Imaging 1999;9:274–279.
30. Hecht EM, Holland AE, Israel GM, et al. Hepatocellular carcinoma in the cirrhotic liver: gadolinium-enhanced 3D T1-weighted MR imaging as a stand-alone sequence for diagnosis. Radiology 2006;239:438–447.
31. Hussain HK, Syed I, Nghiem HV, et al. T2-weighted MR imaging in the assessment of cirrhotic liver. Radiology 2004;230:637–644.
32. Kelekis NL, Semelka RC, Worawattanakul S, et al. Hepatocellular carcinoma in North America: a multiinstitutional study of appearance on T1-weighted, T2-weighted, and serial gadolinium-enhanced gradient-echo images. AJR Am J Roentgenol 1998;170: 1005–1013.
33. van den Bos IC, Hussain SM, Dwarkasing RS, et al. MR imaging of hepatocellular carcinoma: relationship between lesion size and imaging findings, including signal intensity and dynamic enhancement patterns. J Magn Reson Imaging 2007;26:1548–1555.
34. Matsui O. Imaging of multistep human hepatocarcinogenesis by CT during intra-arterial contrast injection. Intervirology 2004;47:7.
35. Yu JS, Chung JJ, Kim JH, Kim KW. Fat-containing nodules in the cirrhotic liver: chemical shift MRI features and clinical implications. AJR Am J Roentgenol 2007;188:1009–1016.
36. Ueda K, Matsui O, Kawamori Y, et al. Hypervascular hepatocellular carcinoma: evaluation of hemodynamics with dynamic CT during hepatic arteriography. Radiology 1998;206:161–166.